Identification of dust transport patterns and sources by using MODIS: a technique developed to discriminate dust and clouds

Zaib un Nisa*

Institute of Geographical Informational Systems (IGIS),
National University of Science and Technology (NUST),
Sector H-12, Islamabad, Pakistan
Email: zaibunnisa12@igis.nust.edu.pk
and
Department of Biology and Environmental Science,
Allama Iqbal Open University (AIOU),
Sector H-8/4, Islamabad, Pakistan
Email: zaib.nisa@aiou.edu.pk
*Corresponding author

Salman Atif

Institute of Geographical Informational Systems (IGIS),
National University of Science and Technology (NUST),
Sector H-12, Islamabad, Pakistan
Email: salman@igis.nust.edu.pk

Muhammad Fahim Khokhar

Institute of Environmental Sciences and Engineering (IESE),
National University of Science and Technology (NUST),
Sector H-12, Islamabad, Pakistan
Email: fahim.khokhar@iese.nust.edu.pk

Abstract: This study focuses on exploring the meteorological factors behind dust emergence and spread over Baluchistan in the post-monsoon season, as much of the existing research has been done on spring episodes. With the integration of remote sensing and meteorological methods, efforts were made to explore the relationship of dust storms with land-atmospheric conditions like surface temperature and aerosol optical depth (AOD) in the selected season. To map dust spatial distribution, a cloud-free product of brightness temperature difference (BTD) composite from MODIS terra level 1B emissive bands was prepared and classified using maximum likelihood technique. Two case studies of October 2004 and December 2011 exhibited the short-term cooling effect on the surface due to increased AOD. Dominant synoptic patterns of cold trough front formation with low-pressure centre development over eastern Iran were found as a significant feature of dust mobility towards warmer Baluchistan. Back trajectory analysis revealed that dust from south western Kazakhstan and eastern Europe converged over land of Kyrgyzstan and Tajikistan, which may have instigated its uplift over Helmand Basin. Evidence of a dominant effect of air masses from Middle East, Iran and Iraq was found in post-monsoon dust episodes.

Keywords: environmental pollution; dust transport; dust enhanced composite; aerosol thickness; back trajectories; dust storm meteorology; Pakistan.

Reference to this paper should be made as follows: Nisa, Z.u., Atif, S. and Khokhar, M.F. (2019) 'Identification of dust transport patterns and sources by using MODIS: a technique developed to discriminate dust and clouds', *Int. J. Environment and Pollution*, Vol. 66, Nos. 1/2/3, pp.80–97.

Biographical notes: Zaib un Nisa is a PhD Scholar at Tuscia University, Viterbo, and Researcher at AIOU, working on ecosystem modelling with Department of Bioscience and Territory-Forestry Lab, University of Molise, Isernia, Italy. Her scientific expertise lies in processing remote sensing data to understand the physical processes of the land and atmosphere interactions and how the climate change is affecting natural ecosystems. This paper is solely based on her research done in Master thesis using the RnD fund provided by the NUST University.

Salman Atif is currently an Assistant Professor at IGIS NUST, obtained his PhD in Geography and Natural Environment from Univesité Paris Diderot, France. His areas of interest are natural hazards and disaster mitigation and the effects of South-Asian water politics on the geomorphology of the Indus basin. Additional topic of interest includes geo-visualisation, comprehensive geo-tool integration, remote sensing, GIS and their use in urban and cadastral development

Muhammad Fahim Khokhar is a Professor at IESE NUST. He obtained his PhD in Experimental Physics from University of Leipzig-Germany. He is also the founder of C-Cargo Group at IESE NUST that provides advisory role in air quality management procedures, and in developing cost effective and efficient climate change mitigation and adaptation strategies in Pakistan.

1 Introduction

Dust storms are a serious global challenge for arid and semi-arid regions which degrade their environment and cause socio-economic disruptions in various spheres of life (Gray, 1999). Main dust sources lie in the sub-tropical desert belt 15°N–30°N, famously known as the Dust Belt, starting from the west coast of North Africa, over the Middle East, Central and South Asia to China where rainfall is scanty, and evaporation is greater than precipitation. Southwest Asia is the second most important dust-raising region of the world that transports tons of dust worldwide (Goudie, 2009). There are two specific dust sources in Middle East and Southwest Asia, i.e., Tokar Delta (hyper arid alluvial delta) and Sistan Basin (lacustrine/deltaic area of aridity) connected with Red Sea and Helmand River that carry high silt load (Hickey and Goudie, 2007). Middle Eastern region contains prominent alluvial plains, particularly the Oman Coast, that release dust in response to atmospheric convection and frontal formations in the months of April and May. The frequency of these dust storms increases in summer due to monsoon trough formation over Middle East (Hamidi et al., 2013). The Middle East with its very little annual rainfall of 200–250 mm, is mostly affected by frequent and severe dust storms, followed by Africa and other neighbouring regions like Iran, Pakistan and India (Furman, 2003). They not only affect the aerosol loadings over sub-continent but also disrupt their socio-economic activities (Khokhar et al., 2016; Alam et al., 2014; Gerivani et al., 2011).

Dust in eastern Iran has strong consequences over Baluchistan, northern and central parts of the Arabian Sea (Kaskaoutis et al., 2014a, 2014b). Especially during the summer months, it originates from Sistan basin (see Figure 1) when low-pressure system over South Asia with ridge formation transpires over the Arabian Peninsula and west of Iran (Rashki et al., 2014). Resultantly, small and light dust particles erode, remain suspended in atmosphere for hours and often disperse over large areas with high wind speed of 40–80 km/h (Keramat et al., 2011). High frequency of these storms is a persistent environmental problem with increased aerosol concentrations that has intensified fog formation over dust-exposed regions in Pakistan (Khokhar et al., 2016).

In terms of dust pattern and relative changes in meteorological conditions, many studies explored consequent variations in meteorological parameters along dust blow pattern. Azizi et al. (2012) and Khoshakhlagh et al. (2012) studied synoptic scale dust circulations in west of Iran using National Centers for Environmental Prediction/National Center for Atmospheric Research (NCEP NCAR) data at 1,000 hPa, 850 hPa and 500 hPa. It identified low-pressure centre over Persian Gulf and West of Iran while high-pressure system on Saudi Arabia that pushes dust over west of Iran especially in spring. Thus, in spring and summer season, its point sources are arid zones of Southern Turkey, Iraqi deserts, Syria, North Eastern Saudi Arabia and Kuwait. Another reason is the strong pressure gradients with low-pressure system over southern and central Iran and high-pressure cells over Caspian Sea, facilitating convection/cyclonic movement of wind-blown dust at surface. In addition, high surface pressure and temperature above dry deserts of Iraq and Syria cause dust particles to rise and move by strong dry winds to other areas of Iran and Baluchistan. This pattern of dust transport was identified by back trajectory analysis on Hybrid Single Particle Lagrangian Integrated Trajectory (HYSPLIT) model using global data assimilation system (GDAS) data (Akbary and Farahbakhshi, 2015; Fattahi et al., 2012). Desert dust in Pakistan, India and other South Asian countries also comes from Oman crossing the Persian Gulf and Iran (Kulshrestha and Kumar, 2014).

Since 1999, Baluchistan has been exposed to thick dust storms from Eastern Iran as result of poor regional hydrological management there (Miri et al., 2010). Its frequency was previously low in high flow period when Hamun lakes were filled by Helmand River. After desiccation of lakes in the drought period (1998–2001), Hamun basin became prominent point source of dust. From 1960 to 2005, this region suffered water diversion schemes in the Aral Sea of Turkemanistan. Much of the research is done on causal factors, such as distribution and source tracking in Iran (Alam et al., 2014; Pahlavanravi et al., 2012; Poodineh et al., 2013; Najafi et al., 2014; Hamidi et al., 2013; Najafi and Vatanfada, 2011; Azizi et al., 2012). There was a need to study these factors from the perspective of frequently exposed areas, therefore, study was conducted to find the reason why dust frequently finds its way to Baluchistan. Pakistan has higher annual mean dust frequencies due to its territorial adjacency to the Iranian playas (Giri et al., 2012). Thus, present study focuses on dust penetration and suspension in Baluchistan.

Previously, Hickey and Goudie (2007) traced transport pathway for adjoining regions at Iran-Afghan-Pak border and used MODIS and TOMS aerosol index (AI) to identify point source in the Sistan basin. While in this study, we have particularly discussed dust episodes of post monsoon season and have developed methodology for dust classification.

2 Site description

Baluchistan with its continental semi-arid Mediterranean climate is known to be a drought hit province, where dust storm is not an unusual phenomenon. It is situated in the southwest of Pakistan and has an area of 347,190 km^2 (41% of Pakistan – Figure 1). It borders Iran to the West, Afghanistan to the North, India to the East and the Middle East to the South. About 93% of the province is covered by hilly rangelands, which makes its climate cold and dry. A large area of the province has rocky outcrops and heterogeneous soil composition. Clay and loamy saline soil are found in inland depressions of Hamun wetlands. Chaghai and Kharan are prominent places of hyper-arid environment where rainfall is less than a 100 mm (Goudie and Middleton, 2001). Dust plumes from Iran/Afghan dry salt lake basins (blue polygons in Figure 1) are more hazardous than from desert of Baluchistan itself. They have capacity to release more than 250 kg saline dust per cubic metre in the air containing particulate matter (PM 2.5 and PM 10) (Rashki et al., 2014).

Figure 1 Topographic feature and map of study area of Baluchistan and neighbouring regions (see online version for colours)

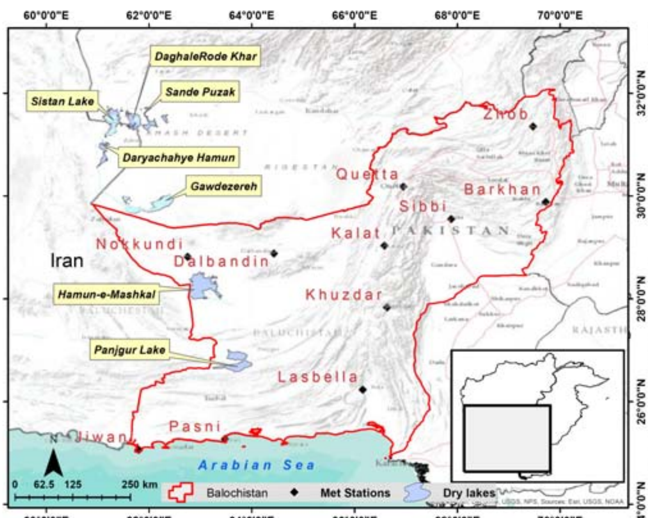

Information Box
Population : 7,914,000 (2011)
Avg. altitude: 2000 feet
Geographical features
mountains (80%)
Dry lakes, deserts and basins (20%)
Climate Semi-arid Mediterranean
Avg. Rainfall: 50-500 mm

Stations	Elevation(m)
Barkhan	1097
Sibi	133
Zhob	1405
Kalat	2015
Khuzdar	1231
Nokkundi	682
Dalbandin	848
Quetta	1626
Sibbi	133
Pasni	6329
Lasbella	87

Note: Diamonds represent the locations of eleven weather monitoring stations, while blue polygons are indicating the dry salt lakes in the region.

3 Methodology

3.1 Datasets used

Monthly occurrence records of dust storms and daily precipitation for 2000–2012 were acquired from 11 meteorological observatories in Baluchistan province (black diamonds in Figure 1). Dust storm images were retrieved from MODIS/terra calibrated radiances 5-min L1B Swath 1 km (MOD021KM) for the years (2001–2013). One image per day was acquired of the daytime overpasses. MODIS sensor is useful in dust detection (Li and Song, 2009) as it possesses excellent propensity of dust monitoring with its multi-spectral bands, wide spectral range (0.4–14.8 μm) and high temporal resolution. For this study, nine dust persistent cases were taken and results of two post monsoon cases are discussed in detail.

Due to unavailability of aerosol robotic network (AERONET) measurement over the study area, daily product of MODIS level 3 aerosol optical depth (Hubanks et al., 2008) at 550 nm resolution (MOD08-AOD550) was used. This product is retrieved from deep blue algorithm that determines AOD for clear-sky snow-free pixels using top of-atmosphere (TOA) reflectance at 412, 470, and 650 nm (in case of deserts, the 650 nm band is only used) over bright surfaces in land. Results by AOD product are reliable considering 0.03 mean error when compared with more than 500 AERONET ground stations worldwide (Ruiz-Arias et al., 2013).

For studying land interactions, six hourly surface temperature data was taken from ERA interim reanalysis (http://apps.ecmwf.int/datasets/data/interim-full-daily). ERA Interim has been chosen due to its comparable spatial resolution with MOD08 product. Features of all datasets used in this study are listed in the Table 1. For meteorological study, geo-potential height, (zonal ‘u’, and meridional ‘v’) wind and surface temperature from six hourly JRA 55 dataset of 1.250 resolutions were used at 900 hPa.

Table 1 Features of remote sensing and meteorological data used in this study

Datasets	*Source*	*Temporal resolution*	*Spatial resolution*
MOD021km-terra	LAADSWEB	Daily	1 km
MOD08	Giovanni	Daily	1°
ERA Interim	ECMWF	6 hourly	1°
JRA55	JMA	6 hourly	1.25°

3.2 Statistical and visual analysis

In the statistical analysis, monthly dust occurrences were compared with annual mean rainfall distribution (record taken from meteorological stations mentioned in Figure 1). Correlation between six hourly temperature data and AOD was computed. Meteorological patterns of dust storms were studied through composite of geo-potential height, (zonal u, and meridional v) wind and surface temperature on grid analysis and display system (GrADs).

3.3 *Dust visual enhancement*

In this study, differences in brightness temperature (BT) of band 20, 29, 31 and 32 are used to extract the dust extent. Brightness temperatures of thermal emissivity bands give useful information for dust detection over land and ocean (Li and Song, 2009; El-ossta et al., 2013).

In storm image analysis, visible (band 3) and thermal infrared bands (20, 29, 31 and 32) of MODIS were pre-processed (geometric and radiometric correction) and their brightness temperature (BT) was calculated through inverse Planck's function given by equation (1) (Markham and Barker, 1986; Prakash and Gupta, 1998; Prakash, 2000).

$$\text{Brightness temperature}(20, 29, 31, 32) = k_2 \Big/ \left(\ln\left(k_1 / L(\lambda) + 1 \right) \right) \tag{1}$$

where $L(\lambda)$ is radiance, $k_2 = C_2/\lambda$, $k_1 = C_1/\lambda$, $C_1 = 1.19104356 \times 10^{-16}$, $C_2 = 1.4387685 \times 10^{-16}$, λ is band specific central wavelength of sensor.

Dust region was not clear in the true colour image (RGB). To clearly identify dust extent, following equations were applied on the images for the visual enhancement of the dust portion.

$$BTD1 = BT3.8 - BT11 \tag{2}$$

$$BTD2 = BT8.6 - BT11 \tag{3}$$

$$BTD3 = BT11 - BT12 \tag{4}$$

where BT3.8 refers to BT of band 20 (3.8 μm), BT8.6 is BT of band 29 (8.6 μm), BT11 is BT of band 31 (11 μm) and BT12 is BT of band 32 (12 μm). A process flow of the methodology used is presented in Figure 2.

Figure 2 Sequence of steps and tools followed in this study for cloud screening and supervised classification of MODIS images

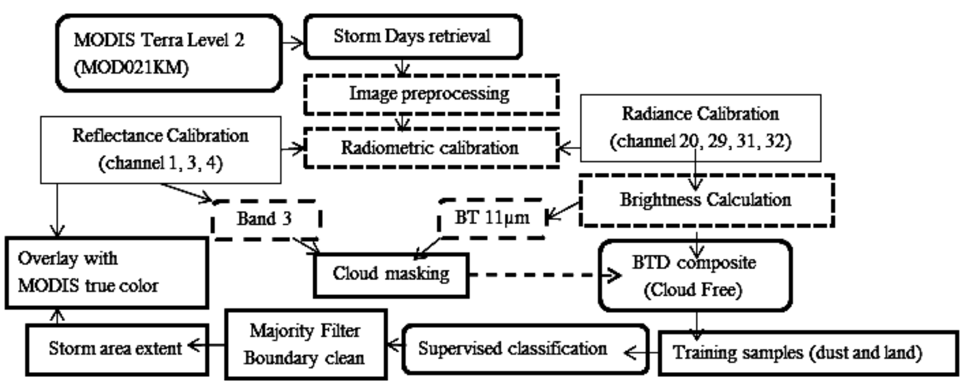

3.4 *Advanced HYSPLIT trajectory analysis*

To examine the origin and pathways of air parcel movements during specific days of an event, three-dimensional ensembles of back trajectories were computed from gridded meteorological data of Climate Diagnostic Center CDC (NOAA) by running physio-meteorological NOAA HYSPLIT model on Real-time Environmental

Applications and Display (READY) online. Generally, a single trajectory is calculated by differential equations nested in Lagrangian trajectory model, as given below (Kulshrestha and Kumar, 2014):

$$dr/dt = v[r(t)] \tag{5}$$

where r(t) is the position vector at time t and v is the velocity field. Different studies have used HYSPLIT backward or forward trajectory analysis to investigate the source and patterns of dust/air pollutant distribution through analysing global data assimilation system (GDAS) (Notaro et al., 2013; Ashrafi et al., 2014), Eta Data Assimilation System (EDAS), final (FNL) meteorological data. In this study, ensembles of back trajectories were calculated in 96 hours back in time for four days on potential temperature, mixed layer, solar flux and humidity starting from altitude of 500 m over Kharan Desert.

4 Results

4.1 Dust detection and classification

Different studies have used different band combinations to detect dust mass. Among them, equations (3) and (4) have been extensively used in desert dust detection. San-Chao et al. (2006) applied thresholds on equations (3) and (4) to detect dust storms in China; it has also been used by Duvall and Ramachandran (2009) and Li et al. (2010) in dust classification. However, Hao and Qu (2007) used reverse combination of equation (4), where positive value of BT12-BT11 showed thick dust storm. Results of BTD composite image of a dust storm event (6 September 2008) is presented in Figure 3. Four samples were taken from BTD composite image for creating spectral profile of desert, clouds, dust and clouds with dust, displayed in Figure 3(c). Spectral response of dust (bold line-square box), clouds with dust (dotted line-triangle), desert (dashed line-circle) and of clouds (dashed dotted line-oval) for three different band combinations was calculated using equations (2)–(4).

BTD between band 20 and band 31 (BTD1) was positive and highest among other BTDs. Spectral profile infers that BTD1 is more effective for discrimination among dust, clouds, and desert. This combination gives information on intensity grades of dust storms (Mei et al., 2008). Nevertheless, increase in difference of BTD2 and BTD3 was observed with increase in dust optical depth. Previously proved, BTD1 gives rough estimation of dust particle elevation over the land (Liu et al., 2011; Li et al., 2007). While, BTD2 can individually discriminate dust from clouds because it shows positive difference for dust while negative for clouds; this contrasting spectral difference can be seen in the example presented in Figure 3(b). It is less affected by surface temperature and gives information on strength of dust storm as well. Moreover, the inclusion of BTD3 helped in discrimination of dust from aerosols. In BTD3, BT of band 31 shows dust top temperature and band 32 shows land surface temperature wherein land surface temperature is always greater than dust top temperature. Studies have shown that difference between BTs of band 31 and 32 is negative when there is dust over land and in case of aerosols it is positive. In this study the difference was negative because dust emissivity is higher in band 32 than in band 31.

Figure 3 (a) True colour image (b) Dust enhanced composite containing symbols of pixel location chosen for spectral profile for respective items (c) Spectral profile for dust, clouds and desert area retrieved from dust enhanced composite (d) MOD35 Cloud mask product in purple colour as reference (e) Masked clouds from MOD visible band 3 (white colour) (f) Dust retrieved as described in the text, of dust storm occurred on 6 September 2008 (see online version for colours)

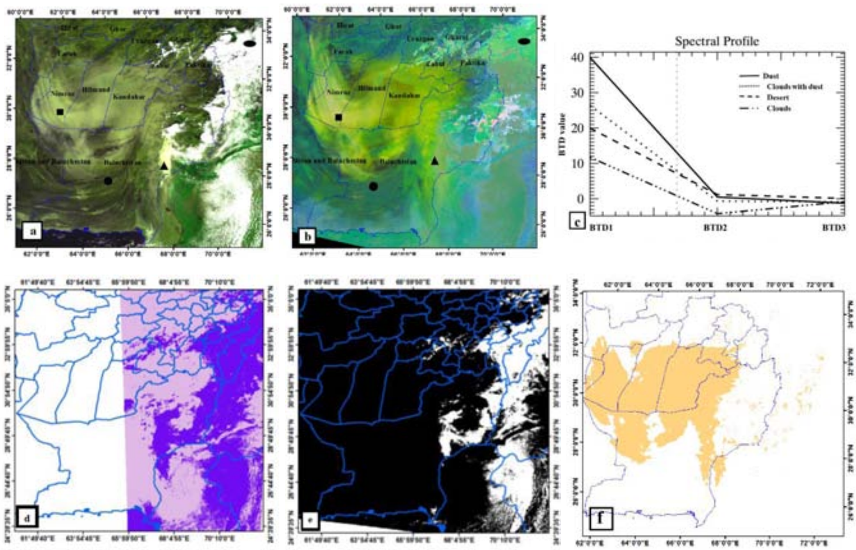

Besides that, cloud screening is an important measure to avoid pixel mixing with dust particles. Clouds were detected from visible band 3 as they showed highest reflection in this band than in any other visible band (1, 2, 4, 5, 6 and 7). A threshold reflectance of >0.3 was applied in screening of low elevation clouds and, BT of band 31 (less than 288 K) was used in masking cirrus clouds. MOD35 cloud mask was also tried but, in this case, the storm area was already cropped, obvious from Figure 3(d). To smoothly classify the dust region, it was necessary to carefully mask the cloud portion first. Thus, threshold over both band 3 and band 31 was used in masking clouds from storm images [Figure 3(e)]. It gave favourable result in dust classification as shown in Figure 3(f). It also indicates that due to intense spectral similarity of both atmospheric features, cloud masking is the necessary step.

Cloud-free product of BTD composite was then classified through maximum likelihood supervised classification technique. After classification, majority filter and boundary clean functions were used to remove spikes in storm boundary. Later, classified dust layers were compared with true colour MODIS image (Figure 3).

4.2 *Monthly dust frequency during 2000–2012*

As mentioned in the previous section, temporal distributions and occurrences of dust incidents were investigated over selected sites during the time period of 2000 to 2012. Records of 11 meteorological stations were analysed by plotting cumulative number of dust events from all weather stations as presented in Figure 4(a). Seasons in Pakistan are largely affected by the monsoon and are defined as, i.e., winter (November to February), pre-monsoon (March to May), monsoon (June to August) and post monsoon

(September–October). Similarly, dust events were separated with respect to their occurrence during different seasons. It is worth mentioning that the frequency of dust events substantially increased during the time period of 2000–2012, especially in the drought period 2002–2005. They were noticeable during pre and monsoon seasons. However, storm frequency was comparatively low in the winter season. During winter, Sistan is influenced by Siberian high-pressure systems and air mass intrusions from the north west and relatively cold northern regions (Rashki et al., 2012a).

Figure 4 (a) Seasonal distributions of total number of dust events form eleven monitoring stations during the time period of 2000–2012 (b) Comparison of average annual rain fall and dust frequency during last 13 years measured at the eleven monitoring stations in the study area (see online version for colours)

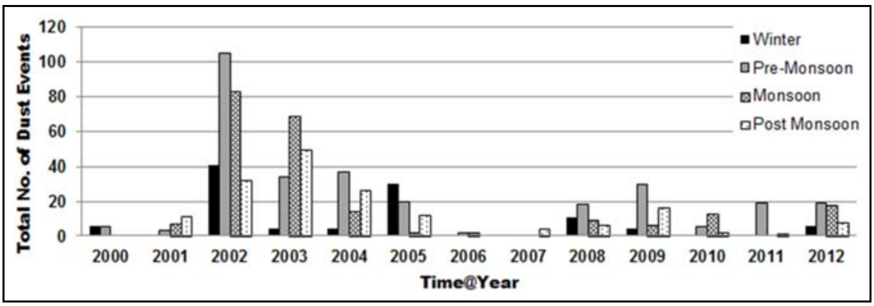

(a)

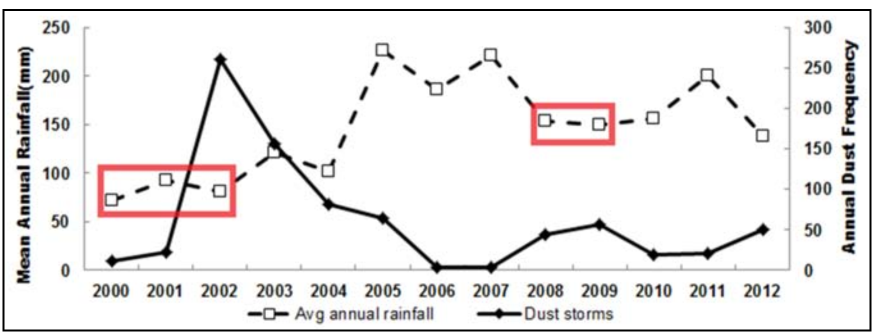

(b)

Note: Red mark is highlighting two drought episodes in Pakistan, i.e., 1999–2002 and 2008–2009.

Stations located in dust path, i.e., Nokkundi, Dalbandin, Jiwanai, Barkhan and Pasni recorded more dust storms because these stations are installed in the southwest of Baluchistan where frequency is noticeably higher than of those in its north and east part. A substantial increase in dust days was observed reaching a maximum during 2002–2004 and a sudden decline in 2006 and 2007 then again greater frequency in 2008–2012. It was further investigated with average annual rainfall (mm), shown in Figure 4(b). An interesting behaviour of increased dust event and decreased rainfall pattern is observed. Rainfall data was obtained from the same meteorological stations used for dust events. Therefore, it may be inferred that observed increase in dust events over study area is linked to dry season experienced during 2002–2004.

Satellite data provided detailed spatial view of dust distribution from its origin. Two main tracks of dust transport were identified from satellite images, i.e., dust from eroded dry beds of Afghan lakes Sande Puzak and Daghl-e-Rodi Khar moved into northeast towards Quetta, Pishin and Qillah Said ullah and were directed further towards Rajasthan. In the other track, Sistan plumes took six to nine hours in approaching Zahedan and sometimes above nine hours to enter the Baluchistan province. Dust plumes from Sistan, Gawadezereh (lowest playa) and Daryachahr e Hamun moved towards Kharan and Chaghai districts and were trapped into hilly terrains of Kharan District while sometimes blew eastward and affected other districts of Panjgur, Kalat and Mastung. Four places specially, Sistan, Sand-e-puzak, Daghl-e-Rode Khar and Daryachehya Hamun are the active sources of dust transport towards Baluchistan (Figure 1). The pressure gradient type, dust storms lasts for longer periods (several hours–few days) whereas convective type lasts for a few minutes to a few hours. Out of 108 storm cases (according to MODIS Terra records), nine dust episodes were severe pressure gradient type dust storms. Their subsidence period varied between dust storms from 5–7 days and has been mentioned against each in Table 2.

Spring-time occurrences are attributed to formation of strong monsoon trough over Sistan-Baluchistan region and Arabian countries which is a main cause of repeated dust storms in May, June and July (Ashrafi et al., 2014). They also identified Syria as point source for dust storms over western Iran (Ahvaz and Tehran). Out of nine subsidence cases, dust episodes in post monsoon season (October 2004 and December 2011) are explored in depth.

Table 2 List of severe dust storm episodes of years 2001–2013, viewed on MODIS

Cases	*Duration*	*No. of days*	*Cases*	*Duration*	*No. of days*
1	1–6 Jun 2001	4	6	4–10 Sep 2008	5
2	9–14 Oct 2001	5	7	11–17 Jul 2010	5
3	20–27 Jul 2003	6	8	18–24 Dec 2011	5
4	12–17 Jun 2004	4	9	2–8 Jun 2012	7
5	5–12 Oct 2004	6			

4.3 Dust episode during October 2004

October is the retreat of monsoon in Pakistan when seasonal low over Baluchistan started to diminish and gave way to the incoming cold advection from Central Asia. In this episode, strong surface winds (15 m/s) protruded into the study area as the low-pressure system developed in the North-East of Baluchistan and created favourable conditions for a dust storm. Slight difference in mobility pattern was observed on 9 October, when dust from dried hamun wetlands was trapped in the south-western Afghanistan and blocked by strips of central Makran Mountains while plumes from dried lakes of Afghanistan moved eastwards from Safaid Koh ranges, funnelled out through Khyber Pass and blanketed Peshawar, Islamabad and Lahore cities with thick veil of dust [Figure 5(a)].

Comparison of aerosol optical depth (AOD) and surface temperature over the study area is presented in Figure 5(b). Significant increase in AOD from 0.2 to 1.4 was found over the region in the presence of thick dust with 3°C decrease in surface temperature. An anti-correlation r = 0.73 was calculated between AOD and surface temperature.

Temperature decreased on 8 and 9 October 2004 when the intense dust layer spread over the study region. This decrease supports the fact that aerosol/dust backscattered the incoming solar radiation, thus causing cooling effect on the surface.

Figure 5 (a) True colour composite MODIS classified dust map (cloud screened and enhanced images) for 6–11 October 2004 (b) Comparison of area averaged MODIS aerosol optical depth (AOD) and ERA interim land surface temperature (2 m) during the dust episode (c) A composite map of wind direction (wind vectors), geo-potential height and air temperature at 900 hPa during dust episode (d) HYSPHLIT ensemble back trajectories analysis was performed for 96 hours form 10 October 2004 at randomly selected location indicated by the black star (see online version for colours)

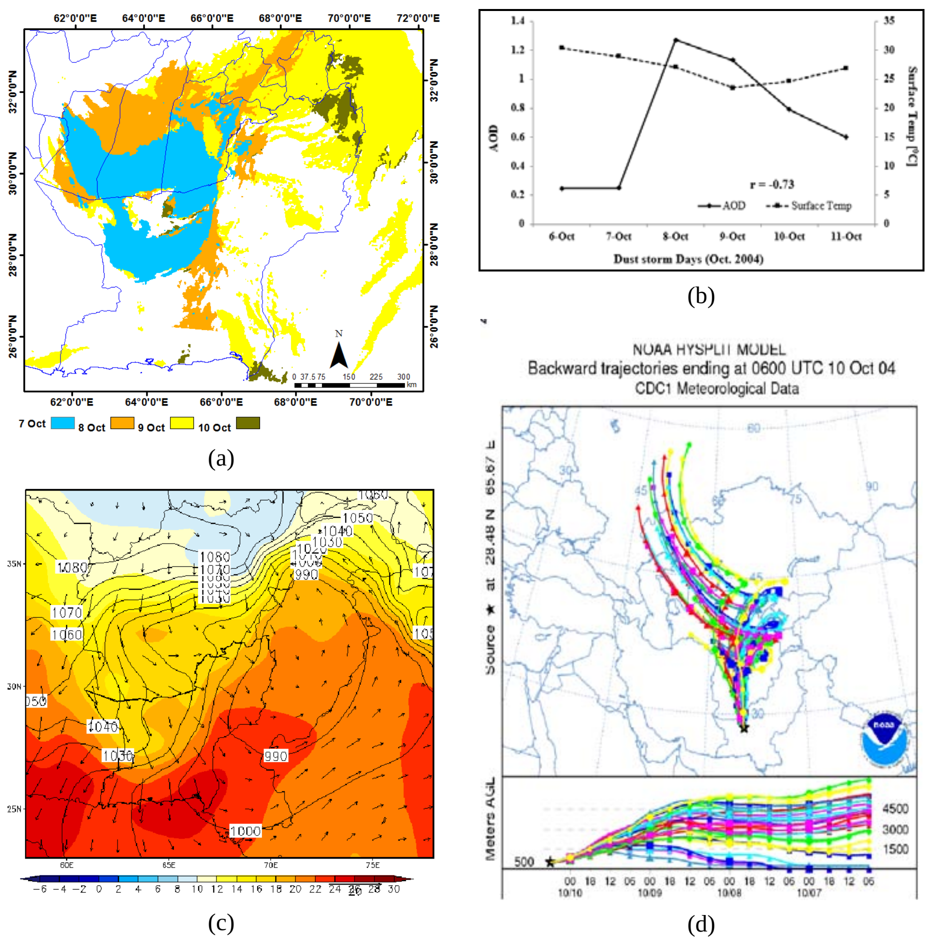

Note: Three different altitudes of 5,000 mAGL, 3,000 mAGL and 500 mAGL were calculated in order to identify the plausible source regions and movement of air masses

Intensified by temperature differences between southwestern Iran and Southern Baluchistan, low-pressure cells formed in the lower troposphere, resulting in the movement of strong winds towards the southeast and developed a strong trough over the region. It initiated convective instability by strengthening of low-pressure centre with sharp geo-potential gradient from 1,060 to 1,000 gpm over eastern Iran and Balochistan, as can be seen from Figure 5(c).

Westerly winds blow and raised fine dust from Sistan basin, resulted into mesoscale gyres (cyclonic circulations) but corresponding cold air intrusion rendered trough to subside with high pressure area dominating the peripheral regions of Baluchistan. Thus, intensification in pressure gradient between southwest Iran and Southern Baluchistan caused cold air advection with subsequent horizontal flow behind cold front and transported large amount of dust masses from Iran, Pakistan and Afghan border towards Nokkundi and Makran coasts [Figure 5(c)]. As a result, massive dust from Dasht e Margo also extended to Quetta, Khyber Pakhtunkhwa and Punjab provinces [Figure 5(a)].

Dust pattern mentioned in Figure 5(c) were further supported by the simulation output of HYSPLIT trajectory models backward in time. Model was run to calculate ensemble of back trajectories at various altitudes of 5,000 metre above ground level (mAGL), 3,000 mAGL and 500 mAGL for 96 hours from 10 October 2004 and onward at Kharan desert indicated by black star in Figure 5(d). Air masses at 5,000 m height AGL reached Pakistan from southeastern part of Russia, crossing over arid and semi-arid regions of Kazakhstan. These westward moving air parcels entered into Uzbekistan, Turkmenistan and Afghanistan. Trajectories at 3,000–4,500 m AGL showed air parcels originate from extreme south of Europe flowing over Caspian Sea swirling back to low land areas of Afghanistan and Pakistan from Kyrgyzstan and Tajikistan. The closest origin of air mass flew above 500 m AGL is dry basin of Helmand River that appeared to make the area more prone to wild storms due to contrast variations in topography of the region. It can be inferred from trajectories, blowing of southwesterly winds over semi-arid dry plateaus of the region made dust advection dominant, thereby affecting AOD concentration in the top of atmosphere.

4.4 Dust episode during December 2011

In the second episode of dust from 19 to 23 December, dust blew from the dry Hamun wetlands and remained suspended over Southwest Afghanistan and Kharan lowlands for four days [Figures 6(a) and 6(b)]. This storm badly affected the transportation network in Afghanistan. A significant increase in the AOD value was found: from 0.25 on 19 December to 0.7 on 22 December 2011 and was decreased to initial levels afterwards [see Figure 6(b)]. A similar, decrease in surface temperature was observed as in case of previous dust episode. A decrease of ~6°C was identified during the consecutive dust days due to lack of surface insolation. An anti-correlation of r = 0.85 was calculated between surface temperature and AOD over the study region.

Winter dust storms in Baluchistan are brought about by cold air advection from the Siberian High, which is a semi-permanent feature. A high-pressure (anti-cyclonic) pattern was observed over the peripheral regions of Baluchistan that intensified when the cold air advection from the Siberian High intruded the western region of Baluchistan. Strong surface winds as a result of strong geo-potential gradients brought about a severe dust storm, which subsided after 4 days as a result of normal surface temperature redemption, ending with a retreat of high-pressure anticyclone towards Persia and weakening of surface winds [Figure 6(c)]. These dust transport patterns were further supported by the simulated back trajectories at three different altitudes of 500, 3,000 and 5,000 mAGL revealed that air masses were present over Kazakhstan, Uzbekistan, Turkmenistan and

Afghanistan before dust entrained into Kharan district [Figure 6(d)]. Dust transport patterns were somehow similar during both episodes, especially before entering the Kharan district of Baluchistan. Trajectories at 500 m heights of both case studies indicate its origin from Russia, Kazakhstan and extreme Eastern Europe. Low-pressure centre and trough formation over eastern Afghanistan are the main causal factor behind frequent dust episodes.

Figure 6 (a) Composite true colour MODIS classified dust map (cloud screened and enhanced images) for 19–23 December 2011 (b) Comparison of area averaged MODIS AOT and era interim land surface temperature (2 m) during the dust episode (c) A composite map of wind direction (wind vectors), geo-potential height and air temperature at 900 hPa during dust episode (d) HYSPHLIT back trajectories analysis is performed for 96 hours from 22 December 2011 at randomly selected location indicated by the black star (see online version for colours)

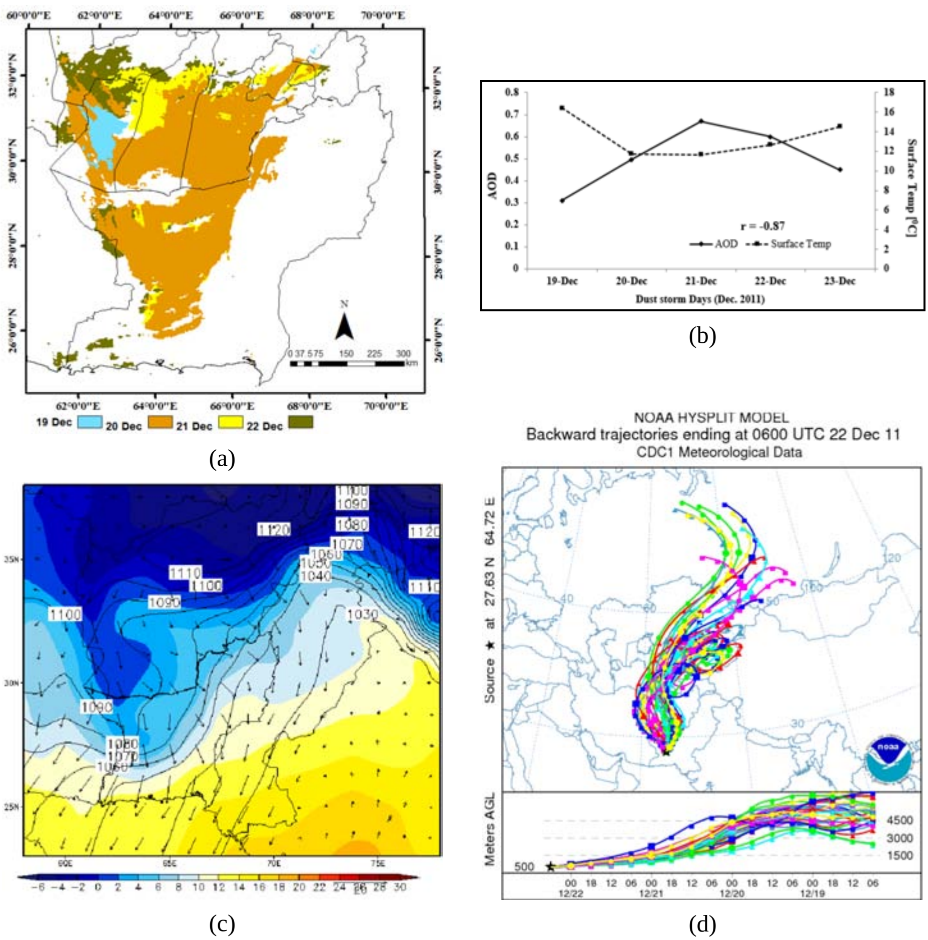

Note: Three different altitudes of 5,000 mAGL, 3,000 mAGL and 500 mAGL were calculated in order to identify the plausible source regions and movement of air masses.

5 Discussions

In years of higher dust frequency (2002–2004), a total of 1.973 million acres of cultivable land was badly affected due to below normal rainfall. Insufficient rainfall and rapid evaporation due to high temperature cause extensive soil loss (Ashraf et al., 2011). Prolonged dry conditions exert significant impact on variability in dust frequency and intensity. Secondly, dust event can be a result of a local storm or it may get transported from a far off place, so its correlation with rain is difficult to justify, however many studies have shown that dust storms in semi-arid regions have negative correlation with rainfall and also are greater in frequency than frequency found in arid regions. Thus, rain can be a limiting factor of dust production (Yang et al., 2007). Zhu et al. (2008) and Aigang et al. (2009) have recognised global warming as another important cause of decline of dust storm. It is negatively correlated with global warming, because increased warming by land/atmosphere weakens surface wind strength and flattens thermal gradient, consequently it makes air circulation stable. Its increasing frequency is also reducing the life of glaciers as dust deposition can reduce albedo and enhance the process of melting by an increased rate of absorption. Mineral dust can reduce cloud particle size and optical depth. Thereby, it may result into lowering of water vapour saturation which acts as a barrier to form droplets. As a result, it decelerates precipitation efficiency and reduces cloud cover particularly over continents that deficits soil moisture and ultimately cause more dust storms (Yin and Chen, 2007).

Furthermore, it can be inferred that saline dust storms in eastern Iran occur by development of pressure gradient between Pakistan (low pressure centre) and high-pressure regime over west-central Asia, as discussed by Kaskaoutis et al. (2014b). Further research is possible on modelling dust storm scenarios at high spatial resolution over the region in order to design a pre-alert system. Besides that, use of windbreakers and sand mulching at the border area may reduce dust penetration. Various studies recommend rehabilitation of hamun wetlands and also emphasise on sustainable hydrological management (Najafi and Vatanfada, 2011). Adoption to these dust preventive strategies can reduce the exposure risk to Baluchistan.

6 Conclusions

This study has primarily emphasised on dust storm suspension reasoning in Baluchistan. Their frequency and seasonal pattern were analysed during the time period of 2000–2012 by exploiting the data from PMD network stations over the study region. It's worth to mention main findings of this study as:

1 the frequency of dust events has shown seasonal trend of greater occurrences in pre-monsoon and monsoon seasons during the time period of 2000–2012

2 bulk of dust penetrated into Southern Baluchistan, is emitted from Sistan basin, about two to three events have its origin from Hamun-e-Mashkal, thus desertification in Iran and Aeolian transport to Baluchistan are the main cause of making its environment drier

3 anti-correlation was observed between clouds/rainfall and occurrence of dust events, mainly due to dry atmospheric conditions in respective years as they exhibited low cloud cover/less rainfall with more dust storms

4 techniques introduced in this study for cloud screening and supervised classification of dust were successfully implemented in order to improve the quality of MODIS images over study area.

During both dust episodes, short-term cooling effect at land surface was identified during the time of high aerosol optical depth (AOD). A maximum decrease of 6°C was observed during the dust episode of December 2011. Moreover, a synoptic system of warm air convergence ahead of cold front and strong cold trough formation over Sistan basin was found as an important feature of dust entrainment into Southern Baluchistan. On broad synoptic scale, transported dust also had its origin from descending air masses of Southwestern Kazakhstan, Uzbekistan, Turkmenistan, Kyrgyzstan and Afghanistan. Transport of dust over Baluchistan from nearby countries (Central Asia, Middle East, Iran and Afghanistan) needs immediate attention of atmospheric scientists and policy makers. Baluchistan also needs to establish air monitoring networks to quantify dust pollutants and its effects on public health, aviation network and agriculture sector. A strong transnational cooperation among vulnerable countries is needed to control dust penetration, drought occurrence, water loss and deforestation.

Acknowledgements

Authors gratefully acknowledge the Japan Meteorological Agency (JMA) for free access to Japanese 55-year Reanalysis (JRA-55) data. We also acknowledge the use of imagery from National Aeronautics and Space Administration (NASA) and ERA interim reanalysis data from ECMWF. We are very grateful to Pakistan Meteorological Department for sharing 11 ground monitoring stations data for dust and precipitation. Also, we acknowledge the provision of NUST RnD funds for MS research to conduct this study.

References

Aigang, L., Tianming, W., Shichang, K. and Deqian, P. (2009) 'On the relationship between global warming and dust storm variation in China', *International Conference on Environmental Science and Information Application Technology, 2009. ESIAT 2009*, July, Vol. 2, pp.59–62, IEEE.

Akbary, M. and Farahbakhshi, M. (2015) 'Analyzing and tracing of dust hazard in recent years in Kermanshah Province', *International Journal of Environmental Research*, Vol. 9, No. 2, pp.673–682.

Alam, K., Trautmann, T., Blaschke, T. and Subhan, F. (2014) 'Changes in aerosol optical properties due to dust storms in the Middle East and Southwest Asia', *Remote Sensing of Environment*, Vol. 143, pp.216–227, DOI:10.1016/jrse.2013.12.021.

Ashraf, A., Naz, R. and Mustafa, N. (2011) 'Evaluating drought impact on vegetation cover of Rarkan Rod-Kohi Area, Balochistan using remote sensing technique', *Pak. Acad. Sci.*, Vol. 48, No. 3, pp.143–150.

Ashrafi, K., Shafiepour-Motlagh, M., Aslemand, A. and Ghader, S. (2014) 'Dust storm simulation over Iran using HYSPLIT', *Journal of Environmental Health Science and Engineering*, Vol. 12, No. 1, p.9.

Azizi, G., Shamsipour, A., Miri, M. and Safarrad, T. (2012) 'Statistic and synoptic analysis of dust phenomena in west of Iran', *Journal of Environmental Studies*, Vol. 38, No. 3, pp.31–33.

Duvall, A. and Ramachandran, R. (2009) 'Intercomparison of candidate methods for mineral dust aerosol classification using MODIS infrared and visible channels', *2009 17th International Conference on Geoinformatics*, August, pp.1–5, IEEE.

El-ossta, E., Qahwaji, R. and Ipson, S.S. (2013) 'Detection of dust storms using MODIS reflective and emissive bands', *IEEE Journal of Selected Topics in Applied Earth Observations and Remote Sensing*, Vol. 6, No. 6, pp.2480–2485.

Fattahi, E., Noohi, K. and Shiravand, H. (2012) 'Study of dust storm synoptical patterns in southwest of Iran', *Desert*, Vol. 17, No. 1, pp.49–55.

Furman, H.K.H. (2003) 'Dust storms in the Middle East: sources of origin and their temporal characteristics', *Indoor and Built Environment*, Vol. 12, No. 6, pp.419–426.

Gerivani, H., Lashkaripour, G.R., Ghafoori, M. and Jalali, N. (2011) 'The source of dust storm in Iran: a case study based on geological information and rainfall data', *Carpathian Journal of Earth and Environmental Sciences*, Vol. 6, No. 1, pp.297–308.

Giri, R.K., Rani, P., Prakash, S. and Singh, J. (2012) 'Satellite viewed dust storms: an overview', *International Journal of Physics and Mathematical Sciences*, Vol. 2, No. 1, pp.38–45.

Goudie, A.S. (2009) 'Dust storms: recent developments', *Journal of Environmental Management*, Vol. 90, No. 1, pp.89–94.

Goudie, A.S. and Middleton, N.J. (2001) 'Saharan dust storms: nature and consequences', *Earth-Science Reviews*, Vol. 56, Nos. 1–4, pp.179–204.

Gray, L.C. (1999) 'Is land being degraded? A multi-scale investigation of landscape change in southwestern Burkina Faso', *Land Degradation & Development*, Vol. 10, No. 4, pp.329–343.

Hamidi, M., Kavianpour, M.R. and Shao, Y. (2013) 'Synoptic analysis of dust storms in the Middle East', *Asia-Pacific Journal of Atmospheric Sciences*, Vol. 49, No. 3, pp.279–286.

Hao, X. and Qu, J.J. (2007) 'Saharan dust storm detection using moderate resolution imaging spectroradiometer thermal infrared bands', *Journal of Applied Remote Sensing*, Vol. 1, No. 1, p.013510.

Hickey, B. and Goudie, A.S. (2007) 'The use of TOMS and MODIS to identify dust storm source areas: the Tokar delta (Sudan) and the Seistan basin (south west Asia)', in Goudie, A.S. and Kalvoda, J. (Eds.): *Geomorphological Variations*, pp.37–57, P3K, Prague.

Hubanks, P., King, M., Platnick, S. and Pincus, R. (2008) *MODIS atmosphere L3 gridded product algorithm theoretical basis*, Document Collection 005, Version 1.1, Tech. Rep. ATBD-MOD-30, NASA.

Kaskaoutis, D.G., Rashki, A., Houssos, E.E., Goto, D. and Nastos, P.T. (2014a) 'Extremely high aerosol loading over Arabian Sea during June 2008: the specific role of the atmospheric dynamics and Sistan dust storms', *Atmospheric Environment*, Vol. 94, pp.374–384.

Kaskaoutis, D.G., Rashki, A., Houssos, E.E., Mofidi, A. and Bartzokas, A. (2014b) 'Meteorological conditions associated with severe dust storms in the Sistan region, Iran', *12th International Conference on Meteorology, Climatology and Atmospheric Physics COMECAP 2014*, May.

Keramat, A., Marivani, B. and Samsami, M. (2011) 'Climatic change, drought and dust crisis in Iran', *International Journal of Geological and Environmental Engineering*, Vol. 5, No. 9, pp.472–475.

Khokhar, M.F., Yasmin, N., Chishtie, F. and Shahid, I. (2016) 'Temporal variability and characterization of aerosols across the Pakistan region during the winter fog periods', *Atmosphere*, Vol. 7, No. 5, p.67.

Khoshakhlagh, F., Najafi, M.S. and Samadi, M. (2012) 'An analysis on synoptic patterns of springtime dust occurrence in West of Iran', *Physical Geography Research Quarterly*, Vol. 44, No. 2, pp.18–20.

Kulshrestha, U. and Kumar, B. (2014) 'Airmass trajectories and long range transport of pollutants: review of wet deposition scenario in South Asia', *Advances in Meteorology*, pp.1–14.

Li, J., Zhang, P., Schmit, T.J., Schmetz, J. and Menzel, W.P. (2007) 'Quantitative monitoring of a Saharan dust event with SEVIRI on Meteosat-8', *International Journal of Remote Sensing*, Vol. 28, No. 10, pp.2181–2186.

Li, X. and Song, W. (2009) 'Dust storm detection based on Modis data', *International Conference on Geo-Spatial Solutions for Emergency Management and the 50th Anniversary of the Chinese Academy of Surveying and Mapping*, September, pp.169–172.

Li, X., Ge, L., Dong, Y. and Chang, H.C. (2010) 'Estimating the greatest dust storm in eastern Australia with MODIS satellite images', *2010 IEEE International Geoscience and Remote Sensing Symposium (IGARSS)*, July, pp.1039–1042,IEEE.

Liu, X., Sun, W., Sun, L. and Li, C. (2011) 'Analysis on the sand-dust source in Mid-Eastern China based on the data of ground stations and RS', *2011 International Conference on Remote Sensing, Environment and Transportation Engineering (RSETE)*, June, pp.4783–4786, IEEE.

Markham, B.L. and Barker, J.L. (1986) 'Landsat MSS and TM post ‐ calibration dynamic ranges, exoatmospheric reflectance and at-satellite temperatures', *EOSAT Landsat Tech. Notes*, Vol. 1, pp.3–8, Earth Obs. Satell. Co., Lanham, Md.

Mei, D.I., Xiushan, L., Lin, S. and Ping, W.A.N.G. (2008) 'A dust-storm process dynamic monitoring with multi-temporal MODIS data', *The International Archives of the Photogrammetry. Remote Sensing and Spatial Information Sciences*, Vol. 37, No. B7, pp.965–970.

Miri, A., Moghaddamnia, A., Pahlavanravi, A. and Panjehkeh, N. (2010) 'Dust storm frequency after the 1999 drought in the Sistan region, Iran', *Climate Research*, Vol. 41, No. 1, pp.83–90.

Najafi, A. and Vatanfada, J. (2011) 'Environmental challenges in trans-boundary waters, case study: Hamoon Hirmand Wetland (Iran and Afghanistan)', *International Journal of Water Resources and Arid Environments*, Vol. 1, No. 1, pp.16–24.

Najafi, M.S., Khoshakhllagh, F., Zamanzadeh, S.M., Shirazi, M.H., Samadi, M. and Hajikhani, S. (2014) 'Characteristics of TSP loads during the Middle East springtime dust storm (MESDS) in Western Iran', *Arabian Journal of Geosciences*, Vol. 7, No. 12, pp.5367–5381.

Notaro, M., Alkolibi, F., Fadda, E. and Bakhrjy, F. (2013) 'Trajectory analysis of Saudi Arabian dust storms', *Journal of Geophysical Research: Atmospheres*, Vol. 118, No. 12, pp.6028–6043.

Pahlavanravi, A., Miri, A., Ahmadi, H. and Ekhtesasi, M.R. (2012) 'The impacts of different kinds of dust storms in hot and dry climate, a case study in Sistan region', *Desert*, Vol. 17, No. 1, pp.15–25.

Poodineh, M.R., Tavousi, T., Negaresh, H. and Alijani, B. (2013) 'Synoptic analysis of storms and severe storms of Zahedan City with an emphasis on predicting the probability of their incidence', *Research Journal of Environmental and Earth Sciences*, Vol. 5, No. 9, pp.537–547.

Prakash, A. (2000) 'Thermal remote sensing: concepts, issues and applications', *International Archives of Photogrammetry and Remote Sensing*, Vol. 33, No. B1, Part 1, pp.239–243.

Prakash, A. and Gupta, R.P. (1998) 'Land-use mapping and change detection in a coal mining area-a case study in the Jharia coalfield, India', *International Journal of Remote Sensing*, Vol. 19, No. 3, pp.391–410.

Rashki, A., Kaskaoutis, D.G., Eriksson, P.G., Qiang, M. and Gupta, P. (2012a) 'Dust storms and their horizontal dust loading in the Sistan region, Iran', *Aeolian Research*, Vol. 5, pp.51–62.

Rashki, A., Kaskaoutis, D.G., Eriksson, P.G., Rautenbach, C.D.W., Flamant, C. and Vishkaee, F.A. (2014) 'Spatio-temporal variability of dust aerosols over the Sistan region in Iran based on satellite observations', *Natural Hazards*, Vol. 71, No. 1, pp.563–585.

Rashki, A., Kaskaoutis, DG., Rautenbach, CJ.W., Eriksson, PG., Giang, M. and Gupta, P. (2012b) 'Dust storms and their horizontal dust loading in the Sistan region, Iran', *Aeolian Research*, Vol. 5, pp.51–62.

Ruiz-Arias, J.A., Dudhia, J., Gueymard, C.A. and Pozo-Vázquez, D. (2013) 'Assessment of the level-3 MODIS daily aerosol optical depth in the context of surface solar radiation and numerical weather modeling', *Atmospheric Chemistry and Physics*, Vol. 13, No. 2, pp.675–692.

San-Chao, L., Qinhuo, L., Maofang, G. and Liangfu, C. (2006) 'Detection of dust storms by using daytime and nighttime multi-spectral MODIS images', *IEEE International Conference on Geoscience and Remote Sensing Symposium, 2006. IGARSS 2006*, July, pp.294–296, IEEE.

Yang, B., Bräuning, A., Zhang, Z., Dong, Z. and Esper, J. (2007) 'Dust storm frequency and its relation to climate changes in Northern China during the past 1000 years', *Atmospheric Environment*, Vol. 41, No. 40, pp.9288–9299.

Yin, Y. and Chen, L. (2007) 'The effects of heating by transported dust layers on cloud and precipitation: a numerical study', *Atmospheric Chemistry and Physics*, Vol. 7, No. 13, pp.3497–3505.

Zhu, C., Wang, B. and Qian, W. (2008) 'Why do dust storms decrease in northern China concurrently with the recent global warming?', *Geophysical Research Letters*, Vol. 35, No. 18, pp.1–5.